We are IntechOpen, the world's leading publisher of Open Access books Built by scientists, for scientists

4,800
Open access books available

122,000
International authors and editors

135M
Downloads

Our authors are among the

154
Countries delivered to

TOP 1%
most cited scientists

12.2%
Contributors from top 500 universities

CLARIVATE ANALYTICS BOOK CITATION INDEX INDEXED

WEB OF SCIENCE™

Selection of our books indexed in the Book Citation Index in Web of Science™ Core Collection (BKCI)

Interested in publishing with us?
Contact book.department@intechopen.com

Numbers displayed above are based on latest data collected.
For more information visit www.intechopen.com

7

Compact, High Brightness and High Repetition Rate Side-Diode-Pumped Yb:YAG Laser

Mikhail A. Yakshin, Viktor A. Fromzel, and Coorg R. Prasad
Science and Engineering Services, Inc.
USA

1. Introduction

Efficient, compact, high average power (100 W and higher) and brightness Q-switched solid-state lasers capable of operating at high pulse repetition frequencies (PRF) of 10 kHz and higher are required for many applications such as material processing, frequency conversion, remote sensing, etc. These lasers represent a scaling up of nearly an order of magnitude over the current generation of diode-pumped solid state lasers. To achieve this level of performance, it is essential to provide a high pump power density in the laser medium, to reduce thermal loads and gradients in active medium and to obtain a good laser beam quality and brightness. Thermal effects in a laser gain medium are generally the main limiting factors for power scaling of diode-pumped solid-state lasers when near diffraction limited output beam is required. Diode-pumped Yb:YAG lasers are a very attractive alternative to the lasers utilizing classical laser material such as Nd:YAG for reducing thermal effects and for scaling the Q-switched output power to the desired level. Yb:YAG has nearly four times less heat generation during lasing than comparable Nd:YAG laser systems [Bibeau et al., 1998, Honea et al., 2000, Rutherford et al., 2001, Goodno et al., 2001] due to a much smaller quantum defect in Yb^{3+}. However, there are two shortcomings with Yb:YAG crystals related to a quasi-three-level nature of its laser transition. The first shortcoming is significant reabsorption at the laser wavelength preventing many laser configurations from being effective. However, recent advances in the development of diffused bonded composite YAG crystals have made it possible to diminish reabsorption losses and achieve a high brightness output. Another drawback is the relatively high level of the laser threshold pump power, which is noticeably, higher than in Nd:YAG lasers. But the last disadvantage is not too important for high average output power lasers, which usually are pumped significantly above threshold. Along with the choice of the gain medium, the important parameters to consider in the design of high power and brightness solid state lasers are the architectures chosen for the diode pumping scheme, laser resonator layout for thermal lensing compensation, energy extraction and cooling of the laser crystal. All of these play critical roles in average power scaling especially when a good quality laser beam is needed. A number of different approaches have been tried by other investigators for developing high power Yb:YAG lasers. Conventional rod lasers allow scaling to high average powers [Bibeau et al., 1998, Honea et al., 2000]**.** But obtaining a good beam quality at high average power is a difficult task due to considerable stress-induced birefringent and

Source: Advances in Solid-State Lasers: Development and Applications, Book edited by: Mikhail Grishin,
ISBN 978-953-7619-80-0, pp. 630, February 2010, INTECH, Croatia, downloaded from SCIYO.COM

a strong thermal lensing in laser rods. Nevertheless, efficient birefringent compensation in an end-pumped Nd:YAG rod laser with CW output power of 114 W and a beam quality value of M^2 = 1.05 has been demonstrated [Frede et al., 2004]. Another approach to development of high power rod lasers was recently demonstrated in cryogenically (~ 77- 100 K) cooled Yb:YAG rod lasers, where 165 W CW output power in near-diffraction-limited (M^2 = 1.02) beam with optical-to-optical efficiency of 76%[Ripin et al., 2004] and even 300 W average power with the M^2 ~ 1.2 and 64% optical-to-optical efficiency has been obtained [Ripin et al., 2005]. But the disadvantage of this laser design is the expensive and rather impractical cryogenic technique.

Traditional zigzag slab geometry, which is known as face pumping [Kane et al., 1984], is more promising than straight-through geometries for scaling to high average power levels while maintaining good beam quality [Koechner, 1999]. However, practical use of slab lasers have been limited by the low laser efficiency that is typically seen in side-pumped slab lasers and by the complexity in engineering a robust, high-power zigzag slab laser system. Modified zigzag-slab laser designs employing conduction cooling and pumping geometry called edge-pumping have been also developed for high power CW and Q-switched Yb:YAG lasers [Rutherford, 2001]. The edge-pumping zigzag slab design eliminates the complexity of the cooling-pumping interface design of the conventional slab lasers, but achieving TEM_{00} mode operation of this laser at high levels of pumping meets is also difficult. Another slab laser design is the end-pumped zigzag slab laser architecture [Goodno et al., 2001]. The slab is pumped from each end by laser diode bars using a lens duct. The diode light is injected through the special coating on the TIR face of the crystal, undergoes TIR reflection from the 45° input face and is guided down the length of the slab. By using a Yb:YAG composite slab pumped from each end by a 700-W laser diode bar stack and an image-inverting stable resonator, 215 W of CW power with linear polarization and average M^2 beam quality of ~ 1.5 was obtained. A constraint of this design for high average power scaling is the considerable energy concentration (pump and intra-cavity fluence) on the small input face of the slab. The thin disk laser design [Karszewski et al., 1998, Stewen et al., 2000] is another approach to high average power lasers. In this laser design, the pump light from a bundle of fiber coupled diodes is imaged onto the center of the thin crystal disk by means of spherical or parabolic mirrors. The pump light not absorbed in the crystal after the first double pass is repeatedly re-imaged onto the crystal. A CW multimode output power of 1070 W at 1030 nm with 48% optical efficiency has been reported in an 8% doped Yb:YAG disk by using of a 16-fold pass through the crystal. This laser design is promising but its disadvantages are a very complicated multi-element optical pumping scheme and a relatively low storage energy because of the small pumped volume of the Yb:YAG crystal that limits the power scaling potential in the Q-switched regime.

In this chapter, we describe the development of compact, side-diode-pumped, Q-switched, TEM_{00}-mode Yb:YAG lasers producing from 65 to 120 W of output power at 10-30 kHz PRF with very high (> 30%) efficiency.

2. Design of the high-average power Yb:YAG laser

Design of the laser configuration, which controls the pumping, cooling and energy extraction, plays a critical role in average power scaling of lasers when a good quality laser beam is required. Achieving high average power in a TEM_{00} output from a Q-switched Yb:YAG laser became possible due to:

1. Proper thermal design of all optical and mechanical components in the laser to: ensure effective heat dissipation from laser crystal using diamond heat spreader plate and limit thermal optical effects, avoid damage to critical components due to overheating;
2. Utilization of flexible multi-pass side-diode-pumping schemes along with a composite laser crystal with low (3%) Yb doped Yb:YAG sandwiched between undoped YAG to uniformly pump the gain region of the laser crystal, and thereby obtain good TEM_{00} mode quality, and efficiently couple pump light from 940 nm pump diodes;
3. Optical thermal lensing compensation to maintain mode stability;
4. Maintaining the energy fluence within the resonator at levels below optical damage threshold;

Below we consider this in details.

2.1 Yb:YAG composite crystal design

A 3% doped Yb:YAG composite crystal with overall dimensions of 3(H) x 10(W) x 21.6(L) mm (doped region is 1.5 x 10 x 10.8 mm) with diffusion bonded clear YAG ends and top plate was conductively cooled from its back and front faces (10 x 21.6 mm) and pumped through the front face by a 250 W CW laser diode bar stack at 940 nm. Figure 1 shows side and top view of this composite Yb:YAG crystal. A back side of the Yb:YAG composite crystal (10 x 21.6 mm) was attached to a copper heat sink through a thin highly thermo-conductive spacer, presumably thin diamond plate. Pumping of the crystal is performed from the top face (10 x 21.6 mm) in multi-pass pumping scheme. To ensure several passes of the pumping beam, a highly reflected coating at 940 nm was introduced on the back side of the crystal. The size of pumping spot on the Yb:YAG crystal was 1.0 x 10.8 mm. Extension of

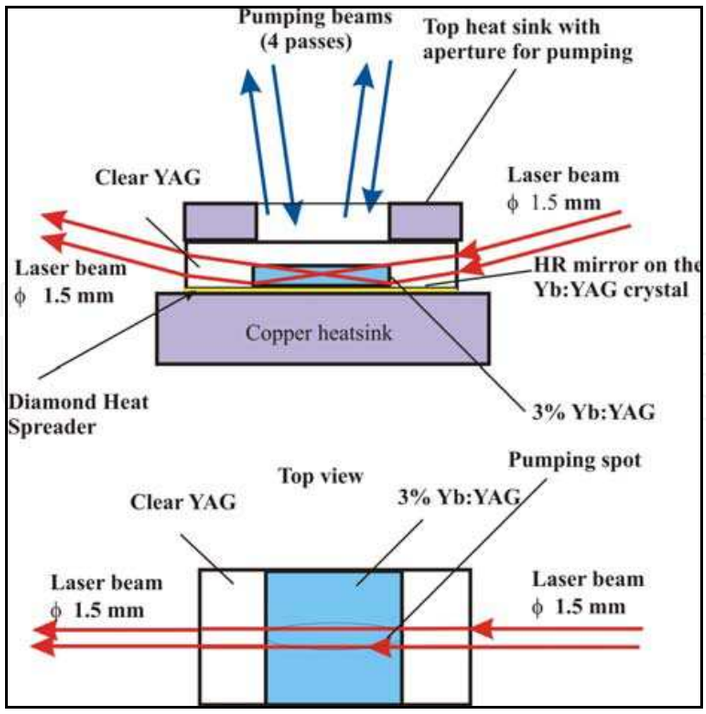

Fig. 1. Side and top views of the composite Yb:YAG crystal. The laser beam executes TIR from the cooled bottom face.

the doped Yb:YAG section of the crystal beyond the pumped width of 1.0 mm to 10 mm provides effective suppression of a spontaneous emission amplification (ASE), that is important for Q-switched operation of the laser.

For scaling up average power of the lasers, proper thermal design of active elements is very important. In order to estimate thermal load and heat distribution in side-pumped composite Yb:YAG crystal showed in Figure 1, we performed numerical calculations using a finite element code (NISA / HEAT III program). It was assumed that the absorbed pump energy in the crystal has uniform distribution over entire pumped volume. The reason for this assumption was the fact that absorption of the pump light at wavelength of 940 nm for one straight pass through the crystal thickness (1.5 mm) was measured to be only ~ 20% from incident beam intensity. Because diode pump beam performed several (4-6) passes through the crystal, the total absorbed pump energy can be considered uniformly distributed. Maximum heat power generated in the crystal is taken as 20 W (~ 10 % of total absorbed pump power).

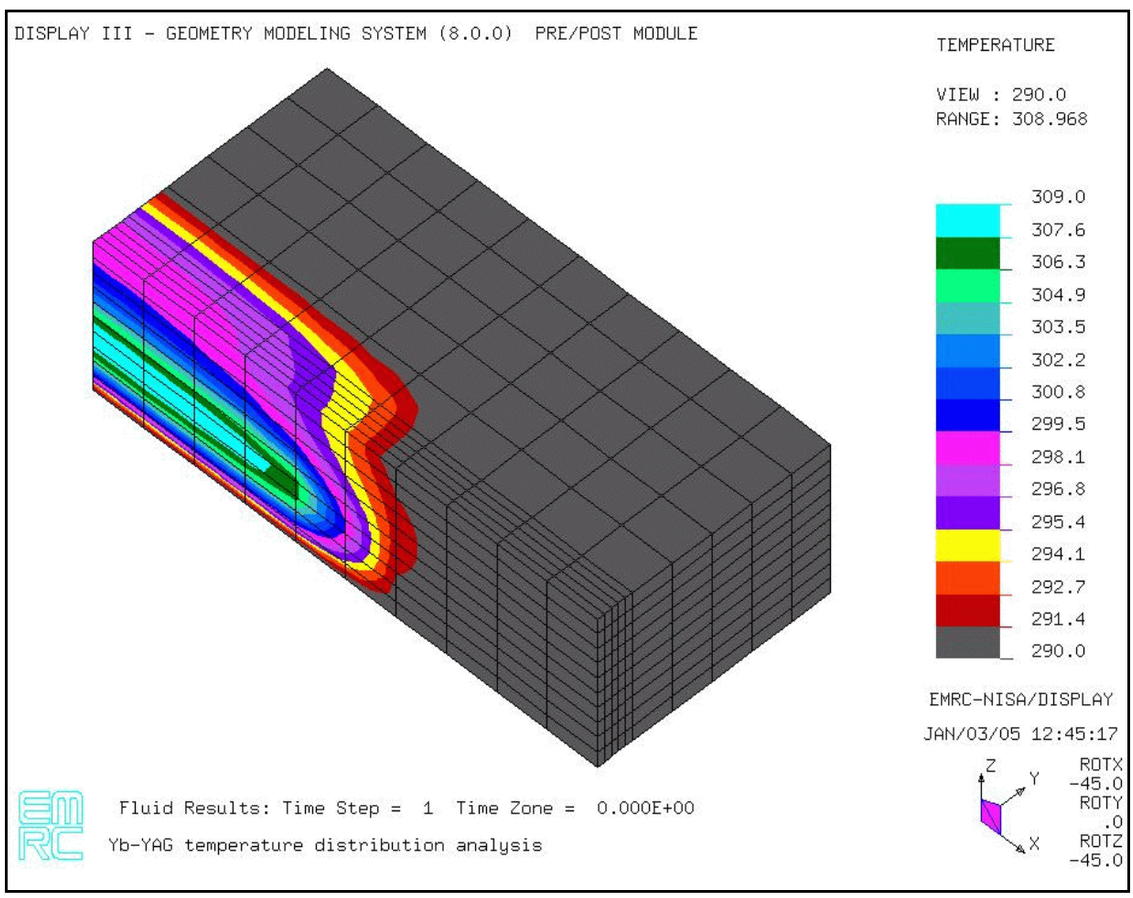

Fig. 2. Temperature distribution in composite 3%Yb:YAG crystal of 3 x 10 x 21.6 mm with homogeneous absorbed pump light area of 1.5 x 1.5 x 10.8 mm, which is cooled from the bottom and from the top faces, except window of 0.22 x 13 mm. Maximum heat power generation in crystal is 20 W. Because of symmetry, only one fourth of the crystal is shown.

Figure 2 shows calculated temperature distribution in the composite crystal with dimension of 3 mm x 10 mm x 21.6 mm, when heat power generation in the crystal is equal to 15 W

(because of symmetry, only one fourth of the crystal is shown). Crystal in Figure 2 is cooled from the bottom and from the top faces (21.6 x 10 mm), except small window of 3 x 14 mm on the top face for pump beam passage. Heat transfer process on the boundaries between crystal and cooling plates assumed to be much faster than inside the crystal. In this case, maximum temperature gradient ΔT between the cooled bottom face and the hottest point in the crystal is ΔT ~ 19°C (see Figure 2). The hottest region of the crystal locates inside top clear YAG part of this composite crystal approximately on 1 mm in depth from upper surface. Because heat transfer speed on the crystal boundaries assumed to be very fast, the temperature of the crystal rises only in limited region around upper window for passing of pumping.

The temperature gradient in the crystal can be divided on two parts: linear growing of the temperature and parabolic temperature distribution. The first part is responsible for appearance of optical wedge in the crystal, while the second part leads to thermal lensing. Knowledge of the temperature gradient arising along the horizontal (along axis Z in Figure 2) and the vertical (along axis Y in Figure 2) planes of the crystal allows to calculate expected focal distance $F_{h,v}$ of the thermal lens in these directions:

$$F_{h,v} = \frac{t_{h,v}^2}{8 \cdot \Delta T_p \cdot (P_t \mp Q_t) \cdot l} \tag{1}$$

where $t_{h,v}$ is characteristic width of the Yb:YAG crystal in the horizontal (h) or vertical (v) direction, respectively; l is the length of the crystal; ΔT_p is the maximum parabolic temperature gradient along the corresponding width t_{hv}, and P_t and Q_t are the thermo-optical coefficients of the YAG crystal (P_t = 87x 10^{-7} K^{-1}, Q_t = 17x 10^{-7} K^{-1}) [Durmanov et al., 2001].

Using equation (1) and calculated temperature distribution in the crystal, expected focal distance of thermal lens at maximum pump level can be estimated as F_h ~ 36 cm in the horizontal plane of the crystal (along the axis Z) and F_v ~ 22 cm in the vertical plane (along the axis Y). However, direct measurements of optical power of astigmatic thermal lenses arising in these crystals (see below) showed that thermal lenses in this Yb:YAG crystal are occurred to be nearly twice stronger than calculated ones. Perhaps, additional heating of the crystal, which exceeds 10% taking into account in the calculation, stems from absorption of the scattering pump light, reabsorption of fluorescence and "non-active" losses in the Yb:YAG crystals (usually ~ 3 - 4 x 10^{-3} cm^{-1}) at laser wavelength.

2.2 Multi-pass pumping scheme

An efficient optical pumping scheme is one of the key elements of the laser design. To improve laser pumping efficiency, we used multi-pass pumping scheme shown in Figure 3, which provided from 6 to 8 passes of the pump beam through the Yb:YAG crystal. This pumping scheme to use the same principle of repeatable passing of the pumping beam through the crystal as that of using in think disk lasers [Karszewski et al., 1998, . Stewen et al., 20001] but our scheme is much simpler. In this multi-pass scheme, a plano-concave spherical focusing lens L_1 (focal length F_1 = 75 - 100 mm depends on diode stack beam divergence) placed in front of the laser diode stack at its focal distance from the pumped Yb:YAG crystal center and a concave mirror M_2 (HR @ 940 nm) with radius of curvature R_2 equal to chosen distance between this mirror and Yb:YAG crystal (available, for example, R_2

= F_1, but not absolutely necessary) placed next to the lens. Second curved mirror M_3 with the same radius of curvature ($R_2 = R_3$) was placed on the opposite side of the diode focusing lens, and its distance from flat reflector M_1 was also taken equal to the mirror radius of curvature.

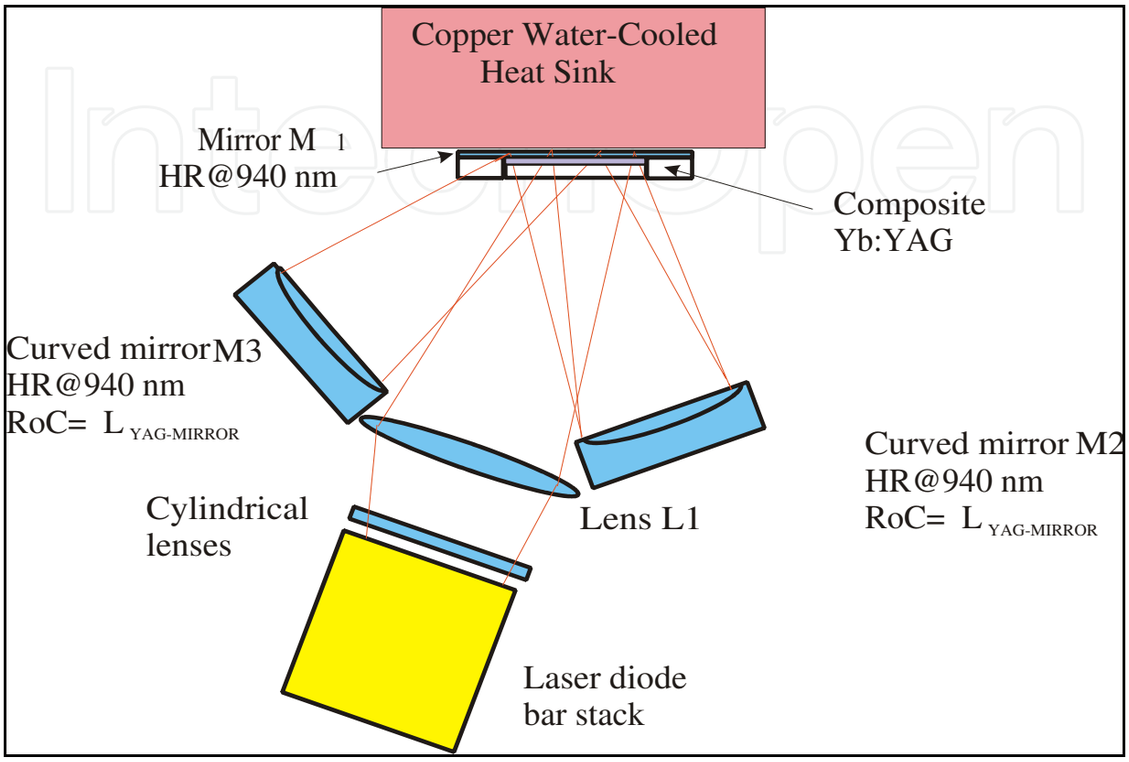

Fig. 3. Multi-pass pumping scheme of Yb:YAG laser

The pumping beam from the laser diode bar stack is focused on the Yb:YAG crystal by a plano-concave spherical focusing lens L_1. The beam is incident on the crystal at a small angle θ_1 (in our experiments, this angle was taken ~ 7°) to the crystal surface. After the first transverse pass through the crystal, the pumping beam is reflected back by a flat mirror M_1 (HR @ λ = 940 nm) located directly on the Yb:YAG crystal. Then it makes the second pass through the crystal, and continues to pass towards the concave mirror M_2 (HR @ λ = 940 nm). This curved mirror is also tilted at some angle θ_2, and thus allows the pump beam to retrace its pass for the third and forth transverse pass through the crystal. The mirror M_2 reflects the pump beam not exactly back as the incident beam is coming, i.e. back to the diode, but instead directs it to the second curved mirror M_3, which in its turn retraces the beam back. As a result, pumping beam performs additional two passes through the crystal. The number of pump beam passes through the crystal can be increased to 8 and even more, if to use a lens with appropriate focal distance in front of Yb:YAG crystal.

Results of comparison of effectiveness of pumping schemes providing two, four and six passes of the pump beam through the crystal are shown in Figure 4. In these experiments, the output pulse energy of the same laser utilizing one or another pumping scheme was investigated. A low PRF (13 Hz) and a simple resonator consisted of a flat output coupler with reflectivity of 0.9 and a curved HR mirror (Roc = 1 m) were used. The length of

resonator was ~ 7 cm. Lower curve shows output pulse energy of the laser, when the pumping beam performed only two passes through the Yb:YAG crystal (mirrors M_2 and M_3 were blocked). Middle curve represents output of the same laser, when four-pass pumping scheme was used (only mirror M_3 was blocked). Upper curve in Figure 4 corresponds to the laser utilizing six-pass pumping scheme. It can be seen from comparison of the lower and the middle curves in Figure 4 that efficiency of the laser increases nearly twice, when pumping beam performs four passes through the Yb:YAG crystal compared with two passes through the same crystal. Utilizing additional two passes of the pumping beam through the crystal, i.e. six-pass pumping scheme, compared with four-pass pumping scheme gives another increase in the laser efficiency of ~ 15%.

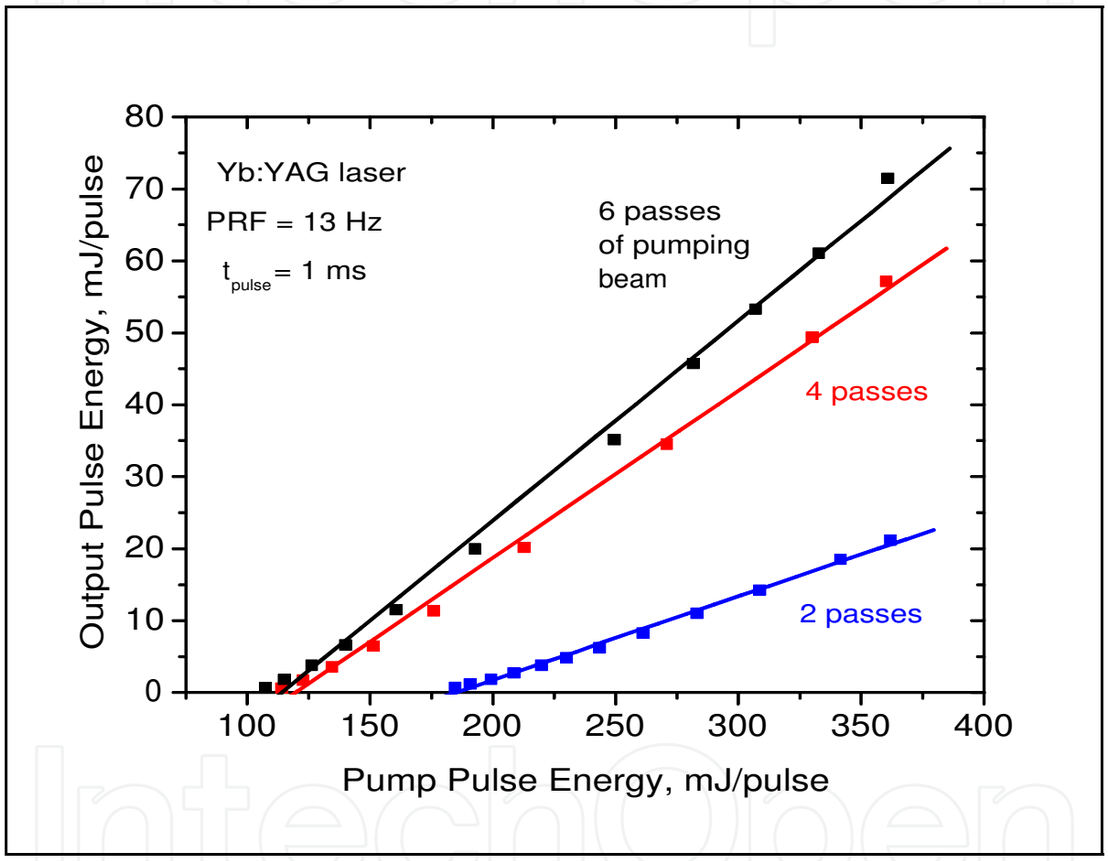

Fig. 4. Output performance of Yb:YAG laser with two-, four-and six-passes of pump beam through the crystal

As it was pointed, the pumped spot size formed by lens L_1 on the Yb:YAG crystal depends on focal distance of this lens and beam divergence of the pumping diode stack in both directions. Varying focal distance of the focusing lens L_1 in front of the diode stack, the size of the pumping spot on the crystal can be optimized. In case of using of the lens L_1 in front of the diode stack with focal distance of 100 mm and mirrors M_2 and M_3 with radius of curvature of 75 mm, the measured pumping beam intensity distribution in the Yb:YAG crystal (for two passes) is shown in Figure 5. It is seen that the pump beam spot has elliptical shape with dimensions of ~ 9.5 mm and ~ 1.1 mm ($1/e^2$ intensity level) in the horizontal and the vertical direction, respectively, and pumping beam size stays nearly

unchangeable, when the distance between focusing lens and crystal is varied on ~ 8 mm. The length of the pumping spot on the crystal increases to 10.8 mm, when all six pumping beam passes are accomplished, while in the vertical plane spot stayed unchangeable.

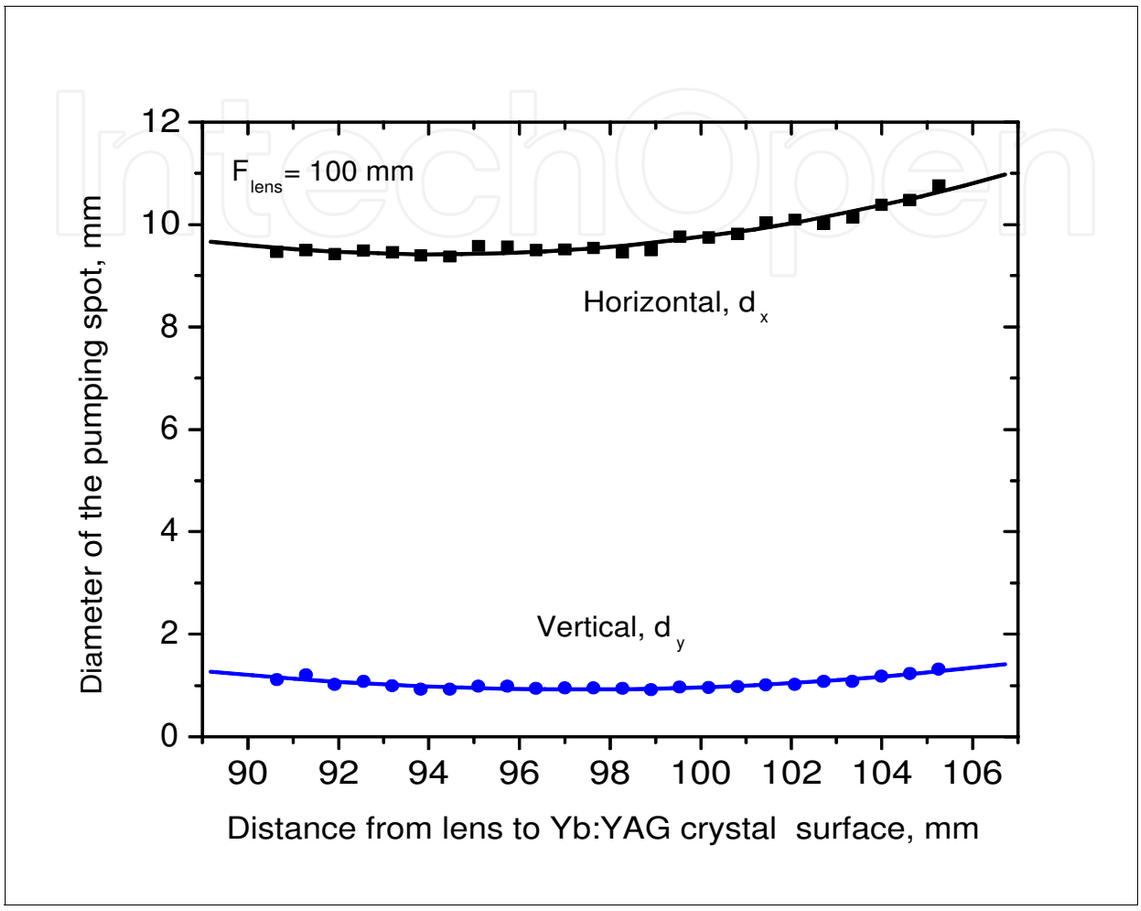

Fig. 5. Measured size of the pumping spot in the composite 3% Yb:YAG crystal in the horizontal and the vertical plane ($1/e^2$ level).

2.3 Yb:YAG single gain module design

To simplify laser design and alignment, Yb:YAG crystal in cooling mount, laser diode bar stack, focusing lens and two HR curved mirrors placed in adjustable mounts have been assembled on the individual base plate forming Yb:YAG gain module. Every such module can be aligned and optimized for the best performance individually in a simple flat-flat resonator.

Figure 6 shows the picture of the assembled gain module. On the right side of the picture, a copper water-cooled mount containing Yb:YAG composite crystal is seen. The crystal with dimensions of 3 x10 x21.6 mm is conductively cooled from the back and the front surfaces. To ensure an efficient heat transfer process between crystal and water-cooled copper heat sink, an optically polished 0.3 mm CVD diamond plate was used as an intermediate heat transfer layer and Yb:YAG crystal was in a direct contact with CVD plate. A 100 μm indium foil used between the front water-cooled heat sink and Yb:YAG crystal surface. On the left

edge of the base plate, a pump laser diode stack is mounted on the adjustable water-cooled manifold. The lens in front of the pump diode stack serves to focus the pumping diode beam on the Yb:YAG crystal. A distance between focusing lens and Yb:YAG crystal is adjusted in order to ensure the pumping spot on the Yb:YAG crystal to be elliptical in shape with dimensions of ~ 9.5 mm and ~ 1.1 mm (at $1/e^2$ intensity level) in the horizontal and the vertical direction, respectively. Gain module plate also includes two adjustable optical-mechanical mounts for two concave mirrors (HR @ 940 nm, radius of curvature F_2 = 75 mm) placed next to the both sides of the focusing lens and used in multi-pass pumping scheme for retracing residual pumping beam back to the Yb:YAG crystal. In the laser resonator, gain module can be rotated on any required angle regarding the axis of resonator without disturbing a crystal pumping system. It is very convenient for building a thermally-compensated multi-component laser resonator.

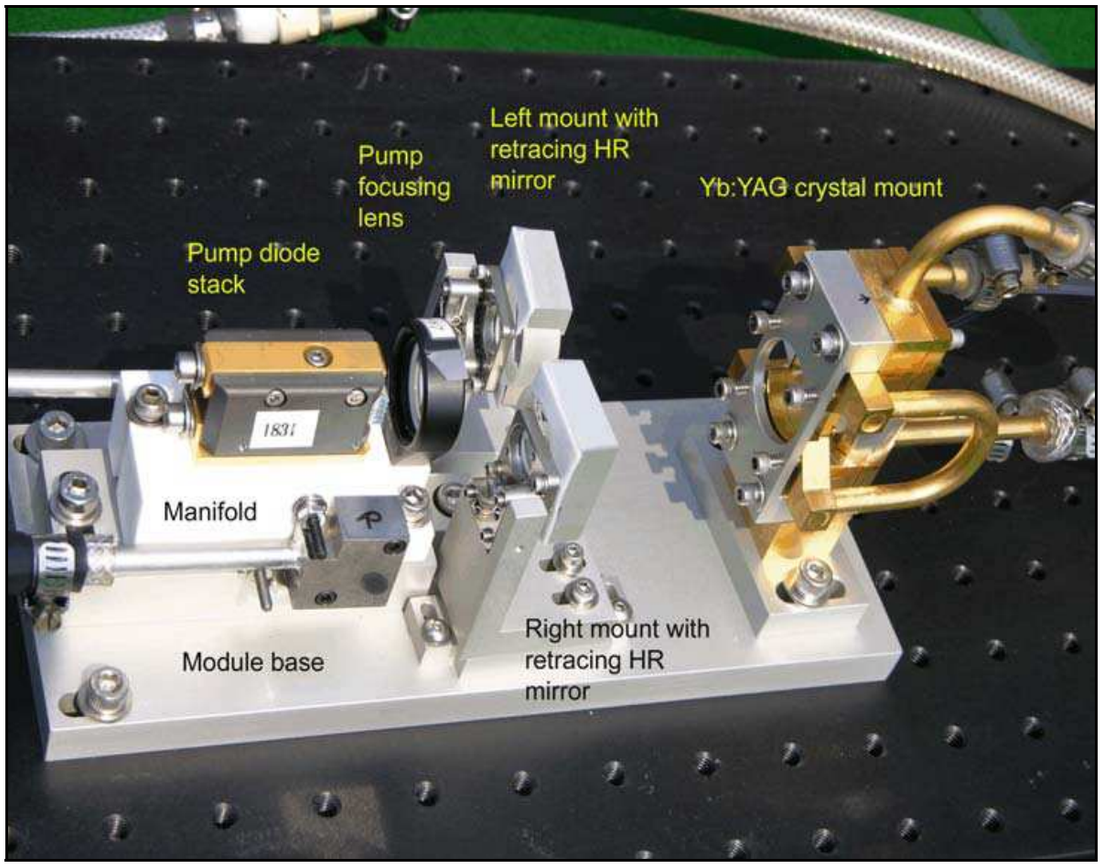

Fig. 6. View of the assembled Yb:YAG gain module

2.4 Measurement of thermal lenses induced in a single Yb:YAG gain module

Accurate measurement of thermal lens induced in our diode-pumped composite Yb:YAG crystal were performed with side-diode pumped gain module shown in Figure 6 and containing a 3% doped composite Yb:YAG crystal. For this purpose, a collimated beam of the probe laser passing through the crystal was used. In front of the crystal, a piece of flat wire mesh having 200 x 200 cells/inch (0.021 mm) was inserted. CCD camera located after the crystal showed a distinct image of this wire mesh along the whole cross-section of the

crystal. When thermal lens was induced in the crystal, initial image was distorted and images of adjacent wire mesh nodes became closer each other because of focusing action of thermal lens. Scanning CCD camera along direction of the probe beam, one can find such position of the camera, where images of adjacent wire mesh nodes are merged in one line. Distance from correspondent principal plane of the crystal to the CCD camera location, where such junction of node images took place, apparently, has to be equal to the focus distance of the measured thermal lens. For astigmatic thermal lens, such merge of images occurs on different distances for the vertical and horizontal directions.

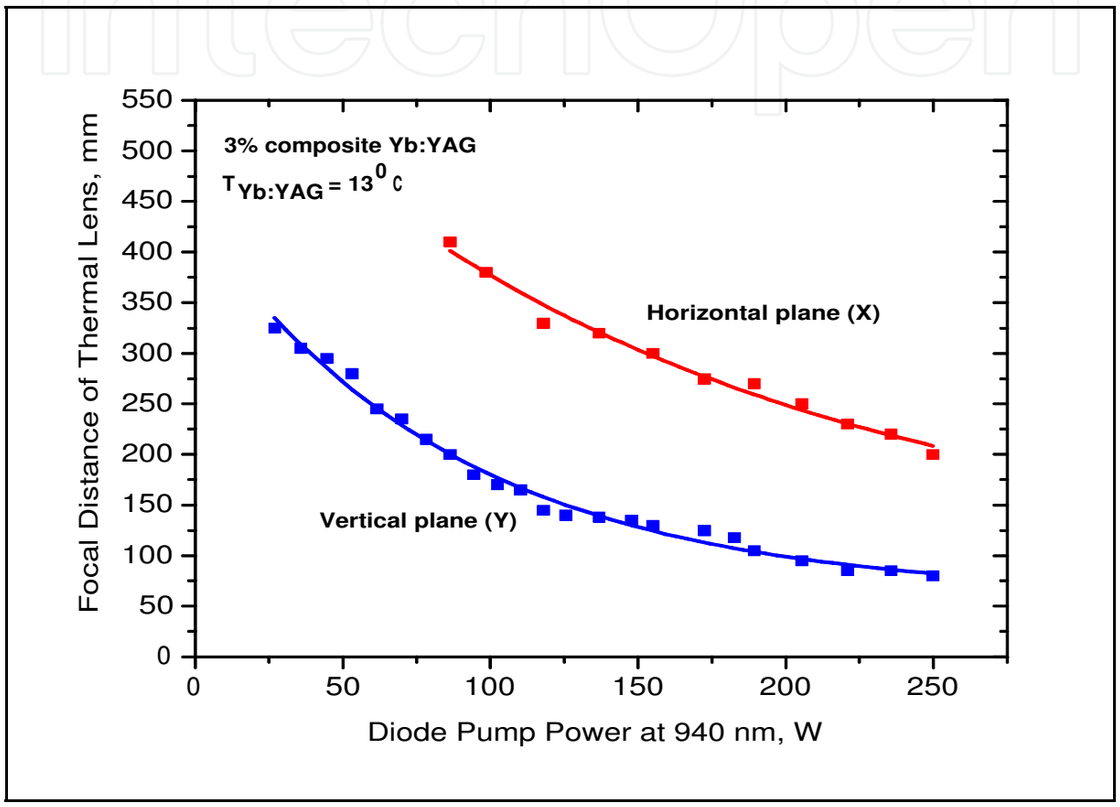

Fig. 7. Measured focal distances of thermally induced lens in side-diode-pumped composite 3% Yb:YAG crystal mounted in the gain module shown in Figure 6.

Figure 7 shows the measured focal distances of thermally induced lenses in the vertical and the horizontal plane of the Yb:YAG crystal (plane XZ and plane XY in Figure 2, respectively) plotted as a function of incident on the crystal pump power. It was found that induced positive thermal lens in this composite crystal is considerable astigmatic and its measured focal power approximately twice bigger than that estimated from thermo-analysis on assumption that 75% of incident pump power is absorbed in Yb:YAG crystal and only ~ 10 % of this pump power is converted in heat in the crystal. At maximum available CW pumping of 250 W, the focal distance of the induced lens in this 3% composite Yb:YAG crystal was measured to be ~ 8 cm and ~ 20 cm in the vertical and horizontal planes, respectively. The difference between the measured and calculated focal powers of thermal lens can be explained by the fact that real heating of the crystal was much higher than that of taking in calculations (10% of absorbed pump power) and maybe also because of possible

arising of additional "electronic" lens due to the excitation of Yb^{3+} ions [Antipov et al., 2006]. With practical point of view, such astigmatic and very short focal distance lens induced in Yb:YAG crystal creates considerable obstacles for development of stable TEM_{00} -mode laser resonator.

3. Performance of the Yb:YAG laser

3.1 TEM_{00} - mode CW performance of one gain module Yb:YAG laser

Experimental investigation of the TEM_{00}-mode operated laser with one gain module and thermally-compensated flat-curved resonator was performed at first in CW regime of operation. It can be noted that the method of compensation of the positive thermally induced lens by means of inserting intra-cavity negative lens or appropriate convex resonator mirrors (or both) can provide TEM_{00}-mode operation only for relatively narrow range of pumping. Parameters of our resonator were calculated in assumption that induced lens compensation will take place around maximum level of pumping - ~ 220 - 250 W.

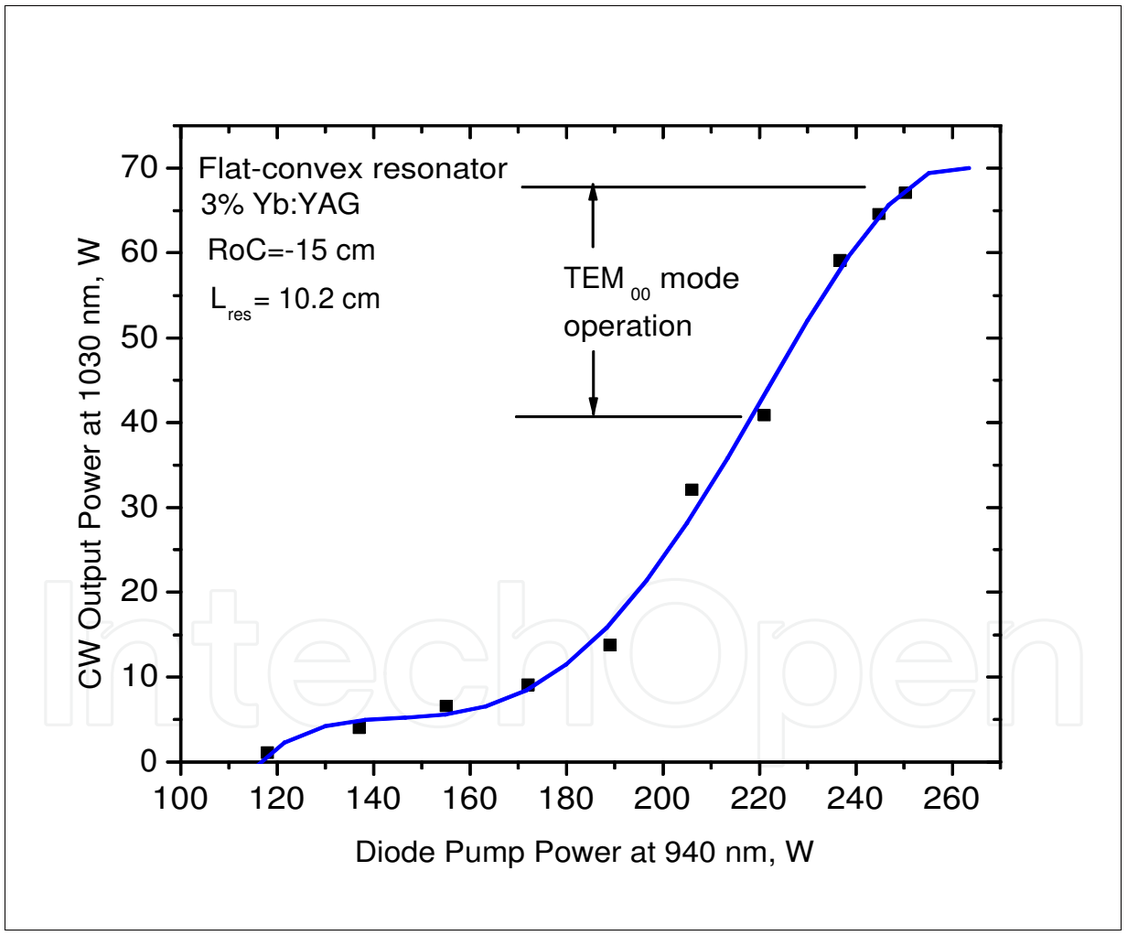

Fig. 8. Output power of Yb:YAG laser with thermally compensated resonator and one composite 3% Yb:YAG crystal in CW regime depends on incident diode pump power.

TEM_{00}-mode operation of this laser in CW regime have been achieved for several tested resonator configurations both containing negative intra-cavity cylindrical lenses and convex

mirrors without lenses. The maximum TEM_{00}-mode output power of the laser for all investigated resonator configurations was in range of 40-67 W. It was found that sensitivity of the resonator to optical alignment increases and TEM_{00}-mode laser output reduces when negative cylindrical lens are used for thermal lens compensation compared with the case of using a convex mirror for the same purposes. It should be noticed that we tried to obtain exact compensation of thermal lens only in the horizontal plane, where laser aperture was larger (~ 1.5 mm). Compensation of the thermal lens in the vertical plane, where it was stronger than that of in the horizontal plane, was not exact especially at maximum available pump power of 250 W, however, laser beam profile in this plane always was very close to TEM_{00} - mode. Figure 8 shows the CW TEM_{00} - mode output of the laser obtained with such simple flat-convex thermally compensated resonator. Resonator was formed by convex HR mirror with radius of curvature of -15 cm placed on ~ 42 mm from the crystal center, and flat output coupler ($R_{1.03}$ = 0.75). The geometrical length of resonator was 10.2 cm. TEM_{00}-mode operation of this laser is observed in the range of pump power of ~ 220-250 W. Increasing of resonator length more than 12.5 cm caused drop in output power and appearance of TEM_{01} and higher order modes. Obviously, that compensation of the thermal lens in the vertical plane became insufficient with increasing the resonator length larger than 12.5 cm. Maximum achievable CW output power of this Yb:YAG laser with thermally compensated resonator in TEM_{00}-mode regime was about 67 W. In multimode regime, maximum CW output power in comparable conditions was ~ 78 W. Figure 9 shows laser beam intensity distribution when laser operates in TEM_{00} mode regime with thermal lens compensated resonator and diode pump power of 250 W. The measured TEM_{00} mode profile shows that the laser output beam is slightly elliptical M^2 ~ 1.3 and ~ 1.5 in the horizontal and vertical directions respectively.

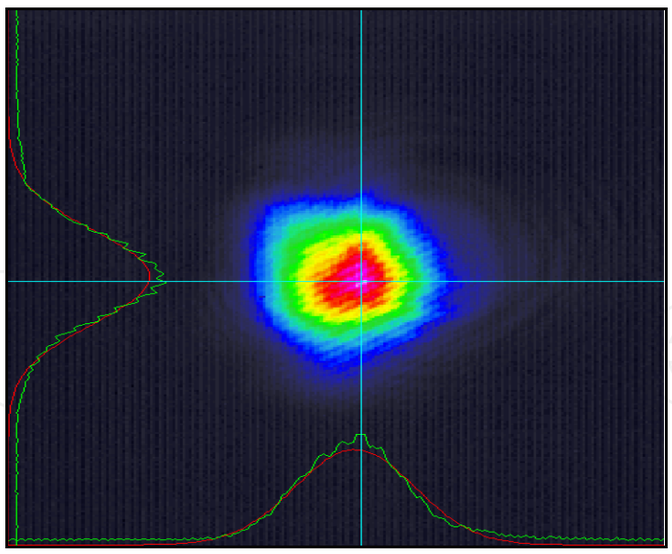

Fig. 9. TEM_{00}-mode beam profile of the CW operated Yb:YAG laser with thermally compensated resonator. Pump power is 250 W, output power is 67.1 W.

3.2 Q-switched performance of one-gain-module Yb:YAG laser

For Q-switched TEM_{00}-mode operation of the Yb:YAG laser with thermally compensated resonator described above, the length of resonator was increased to 130 mm and an

acousto-optical Q-switch (NEOS Technology, model QS27-4S-S) was inserted in the cavity. At the same time, optical length of resonator was only 115 mm, i.e., stayed in the limits defined above for a pure TEM_{00}-mode operation of the laser in thermally compensated resonator. With chosen method compensation of thermally induced lens by means of using not intra-cavity negative lens but resonator mirror with appropriate negative optical power (a convex high reflective mirror with radius of curvature of -15 cm), the laser design looked very compact and simple. A transmission of the flat output coupler was taken of 50% (instead of $R_{1.03} = 0.75$ for CW operation). This transmission was found to be the optimal for Q-switched operation of this laser providing the maximum output and reduction of the intra-cavity flux much below the damage threshold of all optical components of the laser. Figure 10 shows a photo of this bread-board Q-switched laser containing a single Yb:YAG gain module. The back HR concave mirror (R_{oc} = - 15 cm) is separated on 44 mm from the center of Yb:YAG crystal and mounted on a massive base to improve mechanical stability of the laser resonator.

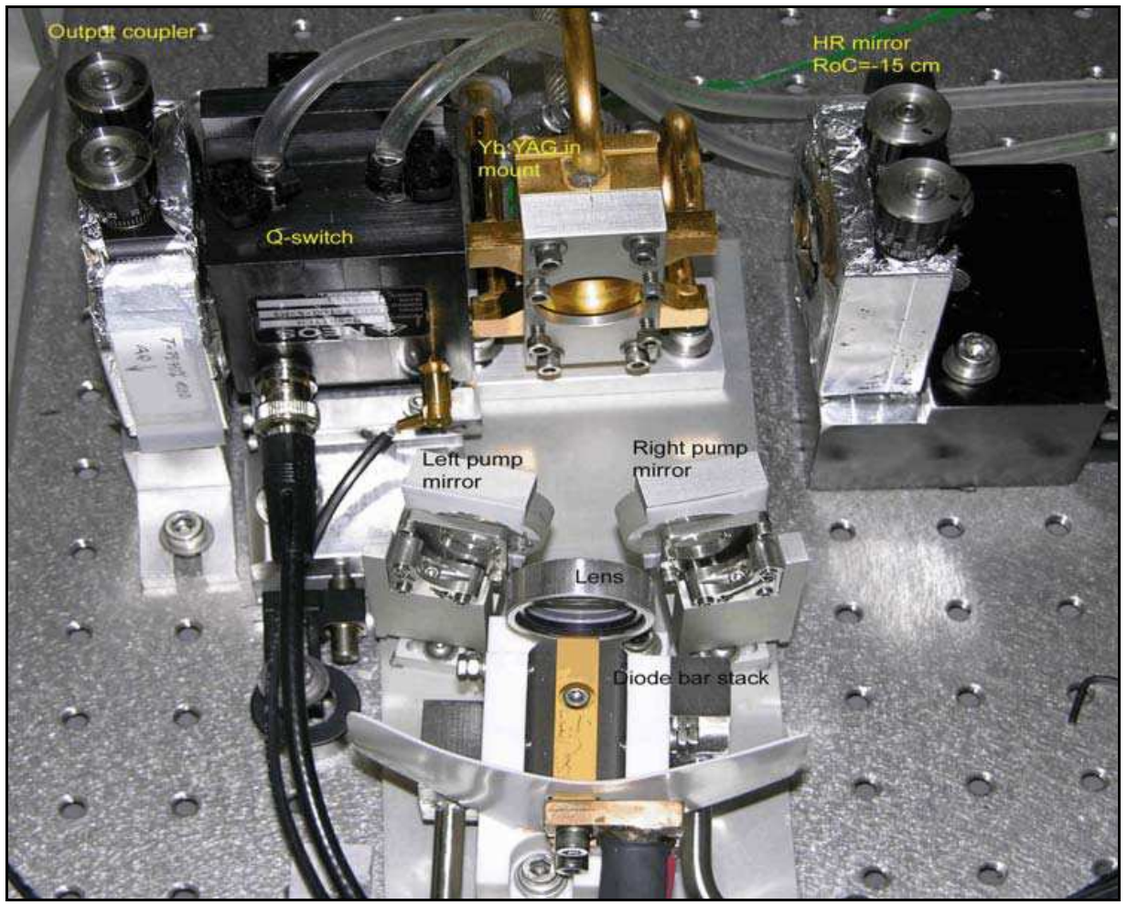

Fig. 10. View of assembled one-gain-module Yb:YAG Q-switched TEM_{00}-mode oscillator.

Figure 8 shows average output power of this one-gain-module laser depends on pump power emitted by diode stack in CW and Q-switched regime at PRF of 10 kHz. It can be seen that in both regimes output power of the laser was nearly the same. The maximum Q-switched output at TEM_{00} mode was ~ 56 W at 250 W of pump power.

Figure 11 shows average output power of this one-gain-module laser depends on pump power emitted by diode stack in CW and Q-switched regime at PRF of 10 kHz. It can be seen that in both regimes output power of the laser was nearly the same. The maximum Q-switched output at TEM_{00} mode was ~ 56 W at 250 W of pump power. Compared to maximum TEM_{00}-mode output of 67 W for similar laser reported earlier, there is ~ 15% reduction of the output for the assembling unit. This reduction is caused, most probably, by slight reduction of absorbed diode pump power because of different spectral width of radiation emitted by different diode bar stacks used in both cases. Some increase in the resonator length due to insertion of Q-switch, in its turn, deteriorates compensation of the thermally induced lens in Yb:YAG crystal in the vertical direction introducing additional diffraction losses. Pulse duration of the laser in Q-switched regime (PRF 10 kHz) gradually reduces from ~40 ns at pump power of 150 W to ~ 20 ns at maximum pump power of 250 W. The TEM_{00}-mode output beam profile in Q-switched regime was slightly elliptical, - bigger in the vertical plane and smaller in the horizontal direction.

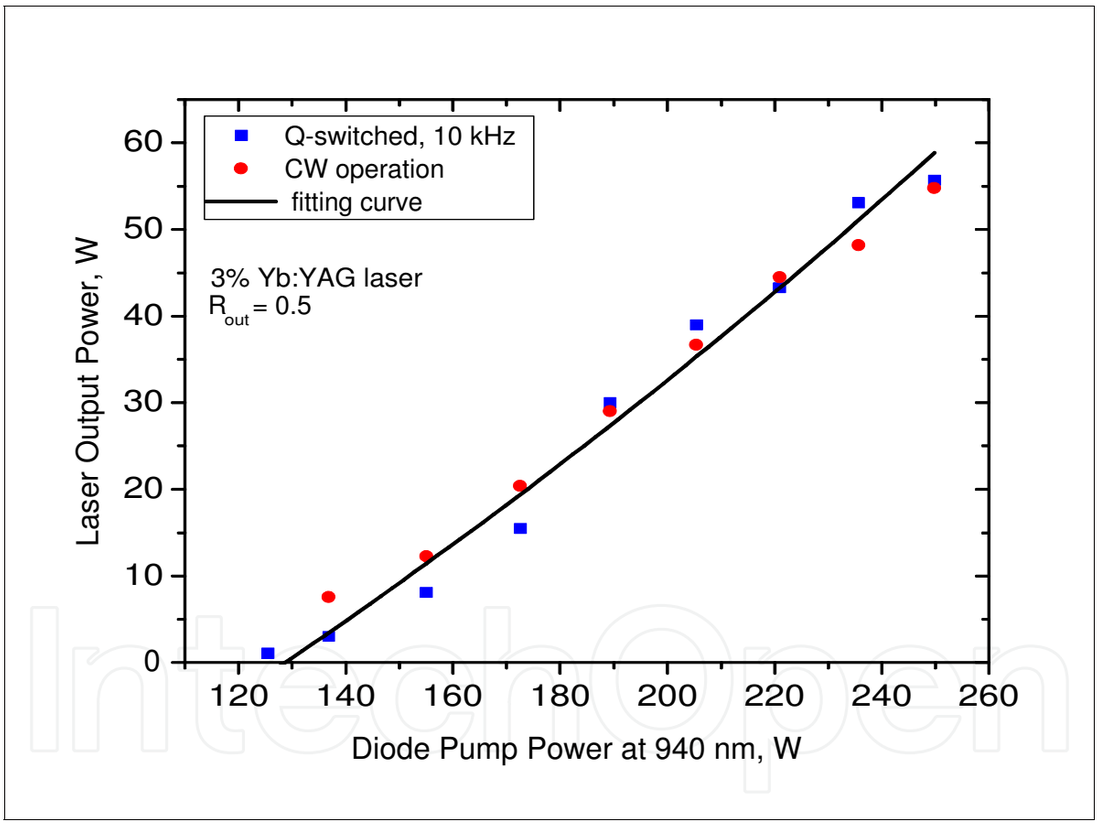

Fig. 11. Output power of assembled one-gain-module Yb:YAG laser with AO Q-switch and compensated resonator in CW and Q-switched regime at PRF of 10 kHz depends on diode pump power.

Thermally induced lens in Yb:YAG crystal permanently changed with increasing of laser pump power. Simultaneously some optical wedge grew in the crystal. That is why resonator of the laser become slightly misaligned with growing of pump power and required to be corrected (usually by means of a small turning of the back HR mirror). As a consequence of that, "cold" and "hot" alignments of resonator were different. During the experiments it was

also found that switching of the laser from CW regime to Q-switched regime was accompanied as well by misalignment of laser resonator because of appearance of optical wedge in acousto-optical Q-switch, when RF power was applied. Transient process of reaching an equilibrium temperature distribution for Q-switch fused silica crystal usually takes ~ 2 -3 minutes because of a big size of this crystal (12 x 30 x 50 mm). Besides, drop in laser output, which was caused by misalignment of resonator, immediately increased heating of the Yb:YAG crystal and produced quantitative and qualitative changes in thermally induced lens and optical wedge in Yb:YAG crystal. All of described above thermal processes created some difficulties for development of safe procedure of tuning on and off the laser and maximization of its pumping, especially in Q-switched regime.

3.3 Performance of the Yb:YAG laser with oscillator- double-pass-amplifier optical schematic

To increase of an average output power of this Q-switched Yb:YAG laser to 100 W, a new laser design employing Power Oscillator- Double-Pass-Amplifier optical schematic was accomplished. The other similar gain module is used as a Double-Pass-Amplifier. Figure 12 shows an optical schematic of this laser. The laser is consisted of two identical side-diode-pumped gain modules. One of them was placed in a simple flat-convex resonator similar to thermally compensated for TEM_{00}-mode resonator used in described above One-Gain-Module Q-switched Yb:YAG laser and served as a powerful master oscillator. The second Yb:YAG gain module is used as a double-pass amplifier. To fulfill two passes of the laser beam through the amplifier, a straight-through and TIR bouncing passes of the incident beam through the Yb:YAG crystal were carried out. Redirection of the laser beam back into amplifier after the first pass was performed by two HR flat turning mirrors. Advantage of using such laser system design is not only in obtaining of a good laser beam quality, but also in reducing of intra-cavity fluence compared with possible design of this laser, when two Yb:YAG gain modules are placed in a common resonator. A distance between two Yb:YAG crystals (in oscillator and in amplifier) and between two successive beam passes through the amplifier is approximately equal to double focal distance of the thermal lens induced in every Yb:YAG crystal in the vertical plane. It means that the laser beam diameter in the vertical plane is re-imaged after every passage it through the crystal. In the horizontal plane,

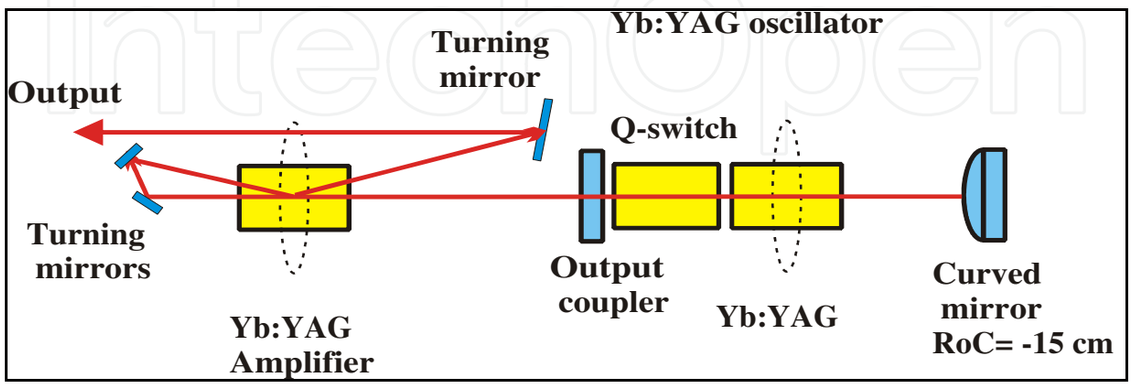

Fig. 12. Optical schematic of two-gain-module oscillator-double-pass amplifier Q-switched Yb:YAG laser.

where initial divergence of the beam was ~ 2.8 x 10^{-3} rad and focal distance of thermal lens in the Yb:YAG crystal was much larger (~ 20 cm)), laser beam diameter after second pass through the amplifier was equal to ~ 1.2 mm and it convergences with an small angle of ~ 3 x 10^{-3} rad. The third turning mirror is used for redirection of the laser beam forward after the second pass through the amplifier. Output laser beam as a whole has TEM_{00} mode profile but different divergence in the horizontal and the vertical planes. To estimate expected performance of the double-pass amplifier, we performed calculations of a small signal gain, α, of this amplifier depends on diode pump power using Franz-Nodvik analysis [Franz & Nodvik, 1963], which takes into account gain saturation on signal fluence. At maximum pump power of 250 W, the average small signal gain was estimated to be ~ 0.55 cm^{-1}. For both laser beam passes, the calculated input beam fluence was below the saturated fluence, which is ~ 9.3 J/cm^2 for Yb:YAG, amounting of ~ 0.44 J/cm^2 for the first pass and ~ 0.73 J/cm2 for the second pass with initially incident average power of 50 W at 10 kHz PRF. The total amplification of Yb:YAG gain module pumped at maximum pump power of 250 W was calculated to be ~ 1.66 and ~ 1.45 for the first and the second passes of the laser beam through the crystal, respectively, when average incident on the amplifier laser Q-switched power was 50 W at PRF of 10 kHz. The total passive energy losses of the laser beam between these two passes were taken as 10%. In these conditions, an average laser output power obtaining from amplifier is expected to be ~ 83 - 85 W after the first pass, and ~ 120-125 W after the second pass.

Figure 13 shows results of experimental measurements of the Q-switched average output power of the described above laser system consisting of Powerful Oscillator and Two-Pass Amplifier at 10 kHz depends on pump diode current (upper curve). Lower curve shows Q-switched average output power of oscillator alone with the same pump diode current. TEM_{00}-mode operation of the oscillator was obtained with high diode current of 70 to 80 Amps (pump power of 220 to 250 W). Maximum Q-switched average power at PRF 10 kHz from oscillator incident on the amplifier was ~ 55 W. After first pass through the amplifier, this average power was increased to ~ 90 W, that is, the maximum amplification for one pass was ~ 1.6. It can be seen that experimental measured value of amplification for the first pass of the laser beam through the Yb:YAG amplifier was very close to the calculated value. After the second pass, 115 W of Q- switched TEM_{00} mode average output power at PRF of 10 kHz have been obtained from this laser system (coefficient of amplification was ~ 1.3). At maximum pumping, Q-switched pulse duration was measured to be ~ 24 ns at 10 kHz and increased to 42 ns at 20 kHz. The TEM_{00}-mode profile of the output beam of this laser was elliptical with larger angular divergence in the vertical direction (where thermal lens in Yb:YAG crystals is stronger). Measured laser output beam quality (after amplifier) showed that in spite of the laser beam is slightly astigmatic but it has nearly TEM_{00} mode profile in both directions - with M^2x = 1.2 and M^2y = 1.33 in the horizontal and in the vertical plane, respectively. In multi-mode operation, laser beam quality of this laser was also comparatively not far from cited above values - measured beam quality was M^2x = 1.7 and M^2y = 1.9, respectively.

4. Conclusion

A compact, high average power, high brightness, diode-pumped Q-switched Yb:YAG laser have been developed. This laser utilized a composite laser crystal with doped Yb:YAG and

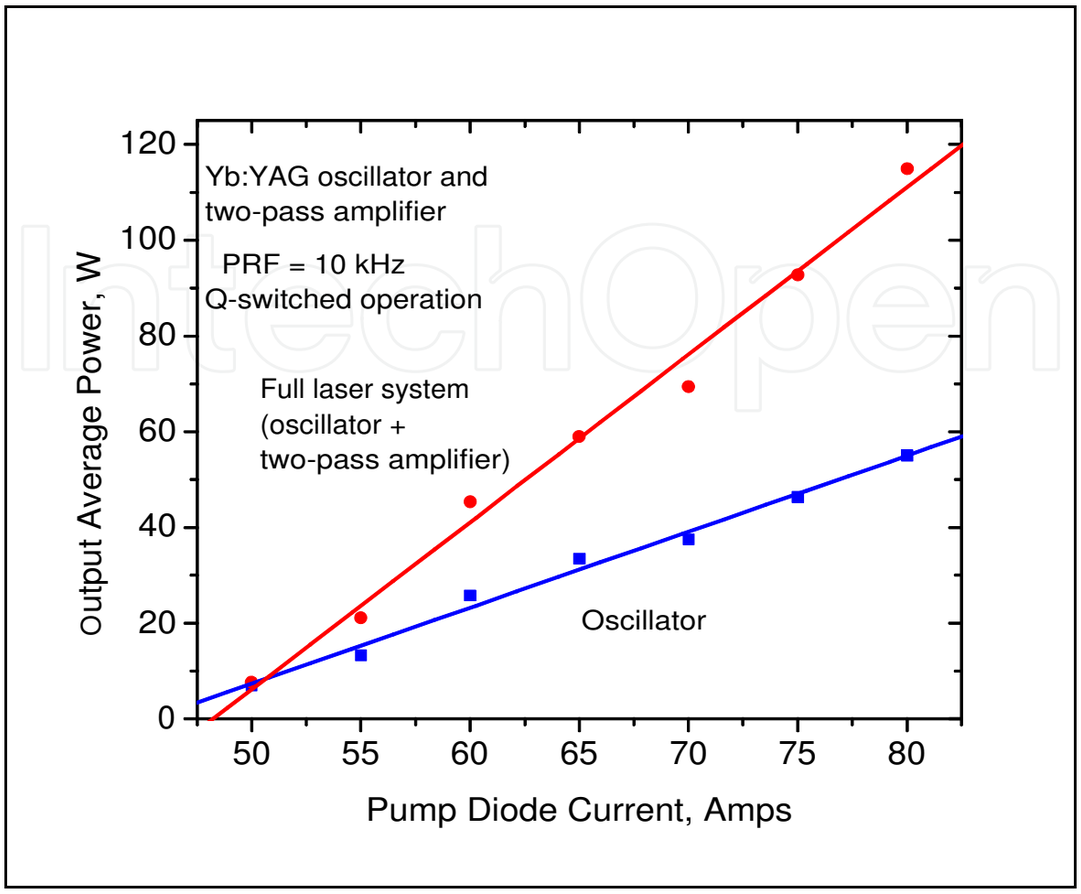

Fig. 13. Output performance of Q-switched Yb:YAG laser employing Powerful Oscillator-Two-Pass Amplifier scheme (upper curve) at PRF of 10 kHz. Performance of the oscillator alone is also shown (lower curve).

clear YAG crystals and an innovative, six-pass side-diode-pumping scheme to couple the 940 nm diode pump beam through a low Yb concentration doped (3.0 atomic %) YAG laser crystal to achieve excellent pump distribution and coupling (> 95%) efficiency. It was capable of delivering 115 W of average output power with a high overall efficiency (> 23% optical), in a nearly TEM_{00} mode (M^2 ~ 1.2) at pulse repetition frequency (PRF) of 10 kHz and pulse duration of ~ 24 ns.

5. Acknowledgements

This research was supported by Air Force Research Laboratory, Kirtland Air Force Base, NM award FA9451-04-C-0152.

6. References

Antipov O.L., Bredikin D.V., Eremeykin O.N., Savikin A.P., Ivakin E.V., Sukhadolau A.V. (2006). "Electronic mechanism for refractive-index changes in intensively pumped Yb:YAG laser crystals", *Optics Letters*, 31, p. 763-765.

Bibeau, C.; Beach R.J., Mitchell, S.C., Emanuel, M.A., Skidmore, J.A., Ebbers, C.A., Sutton, S.B., and Jancatis, K.S., (1998). "High-average-power 1-μm performance and frequency conversion of a diode-end-pumped Yb:YAG laser," *IEEE J. Quantum Electron*, 34, p. 2010.

Durmanov S. T.; Novoselov V.G., Rudnitsky Y.P., Smirnov G.V., Lubimov V.V., Malashko Ya. I., (2001). "Thermo-optic lens in the active element of Nd:YAG lasers and the study of the possibilities of its compensation," *Proceeding of the International Conference on Lasers'2000,* December, 2000 (V.J.Corcoran & T.A.Corcoran, eds.), STS Press, McLean, VA, p.766.

Franz, L.M.; and Nodvik, J.S., (963). "Theory of pulse propagation in a laser amplifier,", 34, p.2346.

Frede, M.; Wilhelm R., Brendel M., Fallnich C., Seifert F., Willke B., and Danzmann K., 2004, "High power fundamental mode Nd:YAG laser with efficient birefringent compensation", *Optics Express*, 12, p.3581.

Goodno G.D.; Palese S., Harkenrider J., and Injeyan H., (2001). "Yb:YAG power oscillator with high brightness and linear polarization," *Optics Letters*, 26, pp.1672-1674.

Honea, E.C.; Beach, R.J., Mitchell, S.C., Skidmore, J.A., Emanuel, M.A., Sutton, S.B., and Payne, S.A., (2000). "High-power dual-rod Yb:YAG laser," *Optics Letters*, 25, pp. 805-807.

Kane, T.J., J.M. Eggleston, and R.L. Byer, (1984). *IEEE J.Quantum Electron.*, QE-20, p. 289.

Karszewski M.; Brauch U., Contag K., Erhard S., Giesen A., Johannsen I., Stewen C., and Voss A., (1998) "100 W TEM operation of Yb:YAG thin disk laser with high efficiency,"*OSA TOPS Vol.*19 *Advanced Solid State Lasers*, Walter R. Bosenberg and Martin M.Fejer (eds.), Optical Society of America, p.296.

Koechner, W, (1999). *Solid-State Laser Engineering*, 5th ed., Springer-Verlag, Berlin.

Ripin D.J.; Ochoa J.R., Aggarwal R.L., and Fan T.Y., (2004). "165-W cryogenically cooled Yb:YAG laser", *Optics Letters*, 19, pp.2154-2156.

Ripin D.J.; Ochoa J.R., Aggarwal R.L., and Fan T.Y., (2005). "300-W cryogenically cooled Yb:YAG laser", *IEEE J. Quantum Electron.*, QE-41, pp. 1274-1277.

Rutherford, T.S.; Tulloch, W.M., Sinha, S., and Byer, R.L., (2001). "Yb:YAG and Nd:YAG edge-pumped slab lasers," *Optics Letters*, 26, pp. 986-988.

Stewen C.; Contag K., Larionov M., Giesen A., and Hugel H., (2000). *IEEE, J. Sel. Top. Quantum Electron*, 6, p. 650.

Advances in Solid State Lasers Development and Applications

Edited by Mikhail Grishin

ISBN 978-953-7619-80-0
Hard cover, 630 pages
Publisher InTech
Published online 01, February, 2010
Published in print edition February, 2010

Invention of the solid-state laser has initiated the beginning of the laser era. Performance of solid-state lasers improved amazingly during five decades. Nowadays, solid-state lasers remain one of the most rapidly developing branches of laser science and become an increasingly important tool for modern technology. This book represents a selection of chapters exhibiting various investigation directions in the field of solid-state lasers and the cutting edge of related applications. The materials are contributed by leading researchers and each chapter represents a comprehensive study reflecting advances in modern laser physics. Considered topics are intended to meet the needs of both specialists in laser system design and those who use laser techniques in fundamental science and applied research. This book is the result of efforts of experts from different countries. I would like to acknowledge the authors for their contribution to the book. I also wish to acknowledge Vedran Kordic for indispensable technical assistance in the book preparation and publishing.

InTech Europe
University Campus STeP Ri
Slavka Krautzeka 83/A
51000 Rijeka, Croatia
Phone: +385 (51) 770 447
Fax: +385 (51) 686 166
www.intechopen.com

InTech China
Unit 405, Office Block, Hotel Equatorial Shanghai
No.65, Yan An Road (West), Shanghai, 200040, China
中国上海市延安西路65号上海国际贵都大饭店办公楼405单元
Phone: +86-21-62489820
Fax: +86-21-62489821

IntechOpen